DETECTION THRESHOLDS IN AUDIO-VISUAL REDIRECTED WALKING

Florian Meyer
Hamburg University of Technology
fl.meyer@tuhh.de

Malte Nogalski
Hamburg University of Applied Sciences
malte.nogalski@haw-hamburg.de

Wolfgang Fohl
Hamburg University of Applied Sciences
wolfgang.fohl@haw-hamburg.de

ABSTRACT

Redirected walking is a technique that enables users to explore a walkable virtual environment that is larger than the extent of the available physical space by manipulating the users' movements.

For the proper application of this technique, it is necessary to determine the detection thresholds for the applied manipulations. In this paper an experiment to measure the detection levels of redirected walking manipulations in an audio-visual virtual environment is described and the results are presented and compared to previous results of a purely acoustically controlled redirected walking experiment.

1. INTRODUCTION

In the design of interactive media environments, it is often desirable to create a virtual space that is larger than the physical space of the reproduction room. For the creation of *walkable* virtual environments, the technique of *redirected walking (RDW)* can be applied to extend the virtual area walkable for the user.

The basic idea is to apply *gains* to the user's turns and walking paths in order to manipulate the physical paths in a way that the user stays within the borders of the physical environment. For a proper immersion into the virtual environment, the applied gains must remain below the user's detection threshold. Our paper reports experiments to determine the detection thresholds of *curvature* and *rotational gains* in an audio-visual virtual environment.

It is generally accepted that vision dominates audition in 3D-orientation of persons (Goldstein [1] cited by Serafin [2]). The open question is, what the consequences for redirected walking (RDW) detection thresholds and thus the possibility to manipulate users' movements are. According to Lackner [3], cited by Razzaque et al. [4], a consistent set of various sensual cues will *increase* the detection threshold of manipulations, i.e., a RDW manipulation is less likely to be detected by the user, and thus larger gains may be applied.

After having previously conducted a purely auditive RDW experiment [5], we now executed the same experiment with an added visual component in order to check the above mentioned hypothesis. This audio-visual RDW experiment and the comparison to the audio-only experiment is the subject of this paper.

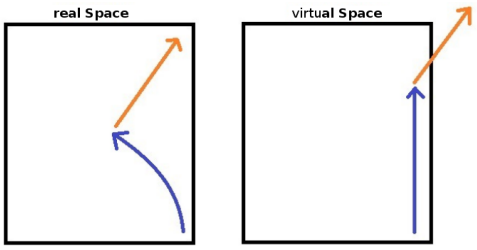

Figure 1: Walking paths in real space and virtual space.

In the following sections, first an introduction to the basic concepts of redirected walking and the current state of research is given. After that, the test procedure and the setup and architecture of the experiment environment is described. Then the results of our experiments are presented and compared to previous results with pure acoustically controlled RDW. Finally, a discussion of the results and an outlook on future work is given.

2. FUNDAMENTALS AND RELATED WORK

This section will give an introduction to the basic concepts of RDW. Various approaches to apply gains to manipulate users' movements are reviewed, and the reported thresholds for the identification of these manipulations are summarized for both visually and non-visually guided RDW.

2.1 General Redirected Walking (RDW)

Humans rely primarily on vestibular, visual and auditory cues for balance and orientation [6], and these cues are also used to distinguish between self-motion (the user moves) and external-motion (the objects around the user, respectively the immersive virtual environment (IVE), move). Under certain circumstances external-motion may be perceived as self-motion, and a consistency of multiple orientation cues may increase that chance [3]. By carefully manipulating the virtual environment (VE), RDW evokes a perceived self-motion of the user, and such provokes an automatic and unconscious self-motion to compensate for the manipulation.

RDW algorithms usually try to steer the users towards the center or the farthest wall of the physical tracking area [7],

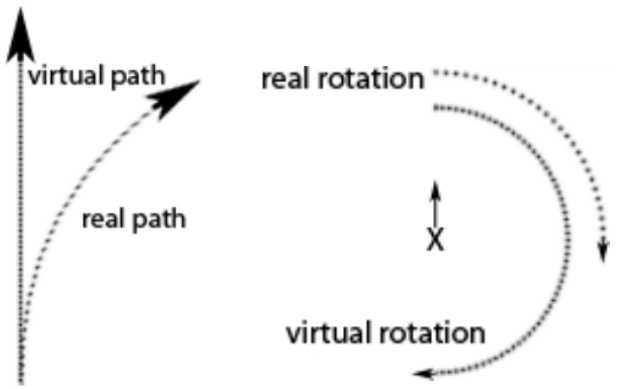

(a) The curvature gain bends a real path into a distorted virtual path. The user unknowingly walks on a curved path.

(b) The rotation gain scales a rotation with the effect that the virtual rotation is greater or smaller than the real rotation.

Figure 2: The curvature gain bends a path and the rotation gain scales a rotation.

while the user is unaware of the steering process and can roam freely. RDW aims at providing the exploration of an infinite IVE within a confined tracking area [8].

2.2 Gains to Manipulate the Users' Movements

While the tracking system constantly provides up-to-date data for the user's physical world position and orientation defined as $P_{physical}$ and $R_{physical}$, the translation is defined by

$$T_{physical} = P_{cur} - P_{pre} \tag{1}$$

where P_{cur} is the current physical position and P_{pre} the previous/last considered physical position. The physical rotation is defined by

$$R_{physical} = R_{cur} - R_{pre} \tag{2}$$

By gains a discrepancy between physical and the virtual movements $T_{virtual}$ and $R_{virtual}$ can be dynamically applied.

A curvature gain stimulates users to unknowingly walk an arc in the tracking area while walking on a straight line in the VE even when they do not intentionally rotate (see figure 2a). A curvature gain g_C is defined by the radius r of the complete circle defined by the curve:

$$g_C = \frac{1}{r} \tag{3}$$

The particular rotational manipulation R_Δ is then calculated by multiplying the physical translation with the curvature gain value:

$$R_\Delta = T_{physical} \cdot g_C \tag{4}$$

R_Δ is then applied to the IVE, but perceived as self-motion by the user.

Rotation gains g_R scale a user's rotation to in- or decrease the amount of a user's virtual rotation $R_{virtual}$ in respect to $R_{physical}$ as illustrated in figure 2b, and are preferably calculated with the rotation of the user's head:

$$g_R = \frac{R_{physical} - R_{virtual}}{R_{physical}} \tag{5}$$

The particular rotational manipulation R_Δ is then calculated by multiplying the physical rotation with the rotation gain value:

$$R_\Delta = R_{physical} \cdot g_R \tag{6}$$

Figure 2b illustrates a rotation gain with a value g_R(-0.5), which up-scales a physical rotation of 90° to a virtual rotation of 180°.

2.3 Experiments for Detecting Thresholds

In March 2008 Steinicke at al. published results of a pilot study [9] within a tracking range of 10m x 7m x 2.5m, in which they identified the following thresholds for visual RDW: Rotations could be compressed or gained up to 30%, distances could be downscaled to 15% and up-scaled to 45%, users could be redirected to unknowingly walk on a circle with a radius as small as 3.3m, and objects and the VE could be down-scaled to 38% and up-scaled to 45%.

The results of different experiments differ greatly though. Other experiments identified thresholds for manipulated rotations at 49% for up-scaling and 20% for down-scaling, as well as a radius for a curved path of 22 meters [10], or 68% for up-scaling, and 10% for down-scaling rotations [11]. The differences in detection thresholds probably correlate with the attention that the test subjects actively pay to the manipulations [10] or other context specific parameters.

2.4 Non-Visual Redirected Walking by Acoustic Stimuli

While a lot of research has been committed to RDW during the last decade, almost all contributions are based upon the visualization of the VE for primary stimuli. Some authors state that the acoustic factor helps users to adjust to the virtual world and that RDW works best, when multiple cues, such as vestibular, visual and auditory, are consistent with each other. This should help the user to perceive external-motion as self-motion [3, 4], and a fully spatialized 3D sound model should be an important component of an IVE for RDW [4]. Even though, the auditory aspect had been paid little attention so far [2].

To the authors' knowledge, Serafin et al. are the only ones who really concentrated on the auditory component of RDW techniques. They conducted two different experiments to determine thresholds for acoustic based RDW techniques [2]. To that goal, they adapted two of the experiments conducted in [10, 11], to be used exclusively with auditory cues. Their experimental setup consisted of a surround system with 16 MB5A Dynaudio speakers in a circular array with a diameter of 7.1 meters and subjects wore a deactivated head mounted display (HMD) to block out their vision. The only audible stimulus in both experiments was the sound of an alarm clock. The sound was delivered

through the speaker array by the technique of vector base amplitude panning (VBAP). In such a setup, VBAP allows the placement of sounds within the circular array of speakers on a plane parallel to the ground level [12].

The first experiment tested the ability to detect rotation gains during rotations on the spot. The second experiment tested the detection of curvature gains while walking on a virtually straight line from one edge of the circular speaker array to a point roughly on the opposite side.

During the first experiment the subjects were asked to turn on the spot towards the sound of the alarm clock. While they were turning, a rotation gain would rotate the alarm clock around the subjects. A rotation gain > 0 would rotate the alarm clock in the same direction the subject is turning, and therefore making it necessary to turn further, to finally face the alarm clock. A rotation gain < 0 would have the opposite effect and result in a smaller physical rotation. When they perceived the sound as in front of them, they were asked whether they perceived the virtual rotation as larger (rotation gain < 0) or smaller (rotation gain > 0) than the physical rotation. The virtual rotation is perceived through auditory cues by locating the position of the sound source, while the physical rotation mainly by the vestibular and proprioception system. During the 22 subsequent trials per test subject, 11 different rotation gains were applied. Each gain was applied twice during the course of an experiment. For the evaluation Serafin et al. also oriented themselves at [10]. Serafin et al. also chose an outbalance of 75% to 25% of the given answers as the detection threshold and these thresholds were reached at gains of 0.82 for greater and 1.2 for smaller responses. This led them to the conclusion, that users can not reliably distinguish between a $90°$ physical rotation and a virtual rotation between $75°$ and $109°$. So users can be turned 20% more or 18% less than the perceived virtual rotation. This range is smaller than a corresponding experiment reported in [10], which can be attributed to the fact, that "[...] vision generally is considered superior to audition when it comes to the estimation of spatial location of objects." Goldstein [1] cited by Serafin et al. [2].

During the second experiment users were asked to walk on a straight line towards the alarm clock. During their movements 10 different curvature gains were applied (each one twice), which led them on an arced physical path and users were asked whether and at which threshold they noticed the direction of the bent path reliably. For this experiment the curvature gain value was defined as the degree the scene rotated after the test subjects walked the whole path of 5 meters. During this experiment the point of subjective equality (PSE) was determined at a curvature gain of -5. The detection thresholds of 75% were reached at gains of -25 and 10 [1] [2]. 25 is roughly equivalent to a circle with a radius of 11.45 meters.

[1] S. Serafin confirmed in personal correspondence that a mistake slipped into the textual representation of the results. Instead of +30, +10 is correct (as the corresponding plot of the paper illustrates)

2.5 Audio-Visual Rotational Gains

The interdependence of acoustical and visual stimuli has recently been investigated by Nilsson et al. [13] for detection thresholds of rotational gains. They conducted experiments *without audio*, with *static audio* (i.e., visual and acoustical targets are primarily lined up, then the gain is only applied to the visual environment), and *moving audio* (i.e., the audio source position moves consistently with the visual scene). The experiments resulted in no significant influence of audition on the detection rates.

2.6 Cyber Sickness

Since RDW manipulates the visual and/or auditory cues willfully and the discrepancy between cues of different senses can lead to different kinds of sicknesses, the consideration and measurement of cyber sickness is part of most experiments regarding RDW.

3. METHODOLOGY AND EXPERIMENTAL SETUP

3.1 Experiment Design

Our experiment for the detection of audio-visual redirected walking was designed ¡¡¡¡¡¡¡ HEAD in close correspondence with our previous audio-only experiment. ======= in close correspondence with our previous audio-only experiment [14]. ¿¿¿¿¿¿¿ release/1.0

To reduce problems with participants suffering from simulator sickness, the range of gains, and such the number of tests were reduced after the first 8 experiment runs.

In the modified experiment design, a complete experiment run for each participant consisted of 44 curvature and 28 rotational gain tests. Ranges of gain values were reduced from $[-1 \dots 1]$ to $[-0.6 \dots 0.6]$ for curvature gains, and from $[-0.6 \dots 0.6]$ to $[-0.4 \dots 0.4]$ for rotational gains. The selection of the test sequence was performed at random by the experiment control software.

Each curvature gain task consisted of the following steps:

1. Participant walks to a corner of the test area (see Fig. 3),
2. participant turns in the direction of one of the adjacent corners,
3. the audio-visual target appears,
4. participant walks towards the audio-visual walking target, while a curvature gain is applied.

These were the steps for a rotational gain test:

1. Participant walks to the center of the room (see Fig. 3),
2. participant turns towards one of the sides of the test area,
3. the audio-visual target appears at $180°$, i.e., directly behind the participant,
4. participant turns towards the audio-visual target, while a rotational gain is applied.

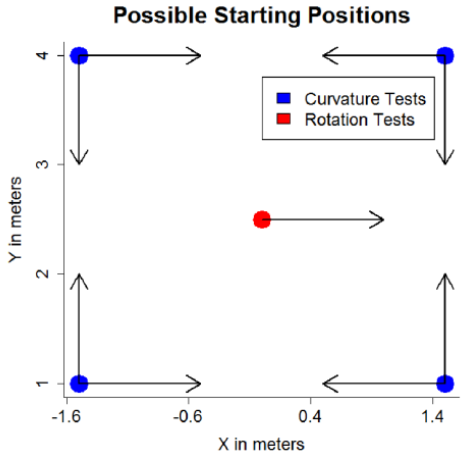

Figure 3: Starting positions for RDW experiments.

Detailed explanations on the design of the test procedure can be found in [14].

To perform the tasks, three simple instructions were given to the participants:

Figure 4: Left: the visual target for walking, right: the visual target for rotation.

1. If you hear or see the *walking target* (see Fig. 4, left), walk towards it, until it vanishes.
2. If you hear or see the *rotation target* (see Fig. 4, right), turn into the direction of the target, until it vanishes.
3. Give feedback ("left" or "right") about the perceived manipulations.

The purpose of the experiment, determination of RDW detection thresholds, was explained to the participants in advance, but neither the participants nor the experiment operator knew the detailed sequence of tests, since they were randomly selected by the test control software. Tests were carried out as *two-alternative forced-choice* tests (2AFC): after each test, the participants only had the choice between the responses "right", indicating a manipulation towards the right-hand side, or "left" for a manipulation to the opposite direction. The answer "no manipulation", or no answer at all was not allowed. In this case the participants had to guess. As a consequence, with no gain applied, the reported left and right manipulations are expected to be equal.

Before and after the experiment, the participants filled a simulator sickness questionnaire according to [15].

Figure 5: The visual virtual environment. The oasis (1), camp (2), pyramid (3), and village (4) are orientation marks. The red circle is the area of user movement.

3.2 System Setup

3.2.1 The Visual Component

The visual component of the virtual environment was designed with Unity [2] for the Oculus Rift DK2 [3]. The scenery is given in Fig. 5. It shows an desert-like area surrounded by distant orientation marks: an oasis, a camp, a pyramid and a village. The red circle in the center indicates the area accessible to the user. It has an diameter of $11\,\mathrm{m}$. To adapt the Oculus Rift to our walking experiments, the Oculus tracking system was substituted by the 3D-tracking system of our lab. Thus the available physical space was a rectangle of approx. $3\times4\,\mathrm{m}$. The computer controlling the Oculus Rift was carried in a backpack by the user as shown in Fig. 6.

3.2.2 The Acoustical Component

The acoustical component serves two purposes: to generate the sounds for the direction of the participants, and to create background noises that provide acoustical landmarks for orientation and for masking of real-world background noises in the lab.

The core part of the acoustic component is a WFS system [16] to create the desired spatial sounds. A very comprehensible overview of the principles of WFS had been given by Spors and Zotter in a tutorial held at the 138^{th} AES convention [17], a thorough analysis is given in the book of Ahrens [18].

The rendering software *sWonder* [4] has been modified by our team to provide proper spatial rendering of focused sources regardless of the participant position [19]. Sounds are played back by a DAW software running on the control computer (see Fig. 7).

The background noises were sounds of flamingos, camels, a campfire, oriental music and wind. The background sounds

[2] http://unity3d.com/
[3] https://www.oculus.com/en-us/rift/
[4] https://github.com/sensestage/swonder

Figure 6: A fully equipped test person with tracking system target (1) and Oculus Rift (2) connected via cable (3) to the control laptop (4).

were rendered as plane waves, arriving from the directions of the visual landmarks.

The controlling sounds for the participants were the sparkling sound of a fountain as *acoustic walking target*, and the sound of a barking dog as *acoustic rotation target*.

3.2.3 System Architecture

The overall system architecture is given in Fig. 7. The system is built with these components:

1. An IR-based tracking system that broadcasts the participant's position via WLAN,
2. the Oculus Rift and its controlling laptop PC carried by the participants in a backpack,
3. a laptop PC controlling the movements of the virtual sound sources,
4. a control computer running these programs:
   - DAW software for sound playback,
   - OSC gateway to the WFS system,
   - communication gateway for the Oculus Rift control PC,
5. the WFS system consisting of a controller PC and two rendering nodes for 208 speaker channels with a spacing of 10 cm forming an rectangle of roughly 5×6 m.

The connections between the laptop controlling the acoustic component (3), the control computer (4), and to the WFS system (5) are wired LAN connections, the other network connections are established via WLAN.

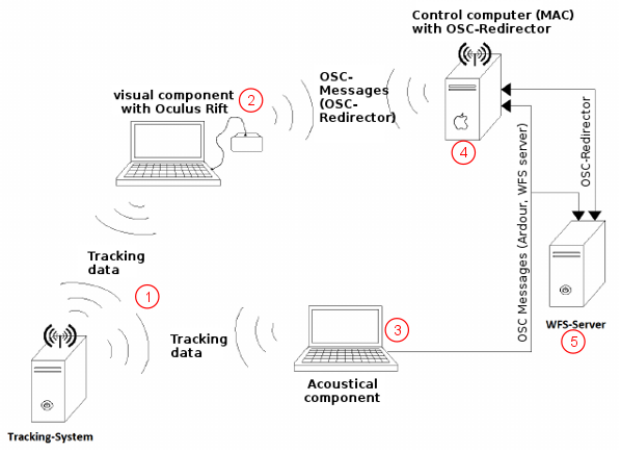

Figure 7: Distributed architecture of the experiment control system. Numbers 1 to 5 correspond to the enumeration given in the text

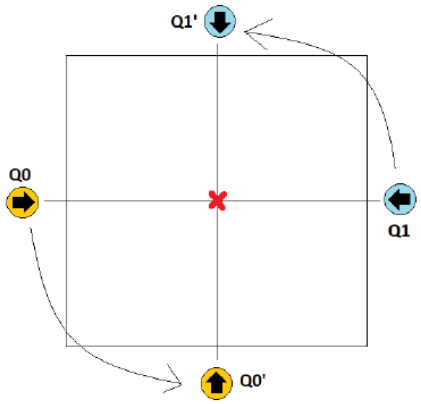

Figure 8: Rotating the acoustical environment.

3.3 Realization of Rotational and Curvature Gains

From our previous acoustical RDW experiments, there existed a fully functional software for the acoustical component to control the test sequences and apply the required gains. Gains are applied by rotating the virtual sound sources synchronously around the participant (see Fig. 8). This is being done by sending appropriate OSC messages to the WFS server via LAN (see Fig. 7). The WFS server offers a data stream with source positions. This stream is subscribed by the visual component to synchronize the visual with the acoustical environment.

4. RESULTS AND DISCUSSION

Our study was carried out with 20 participants, 8 female, and 12 male, most of them students of computer science. Each experiment lasted approximately one hour, with an uninterrupted exposure to the virtual environment of 20 – 35 minutes.

As stated in the previous section, our primary intention was to perform the same series of experiments that were earlier performed with purely acoustically controlled RDW, but it turned out that the participants suffered from severe

symptoms of simulator sickness. Therefore the applied gains were limited to smaller values.

The results are summarized in Fig. 9 for rotational gains, and in Fig. 10 for curvature gains. For the curvature gains, positive and negative gains have been pooled, as there was no significant bias in one of the directions.

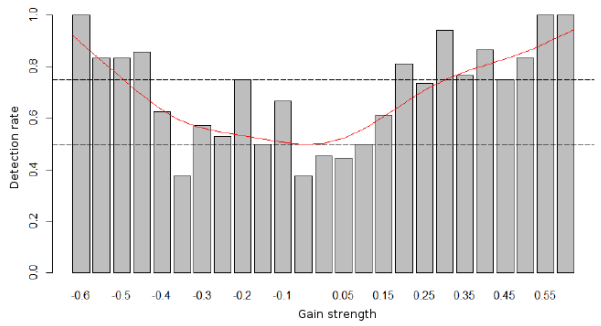

Figure 9: Results of the rotational gain experiments.

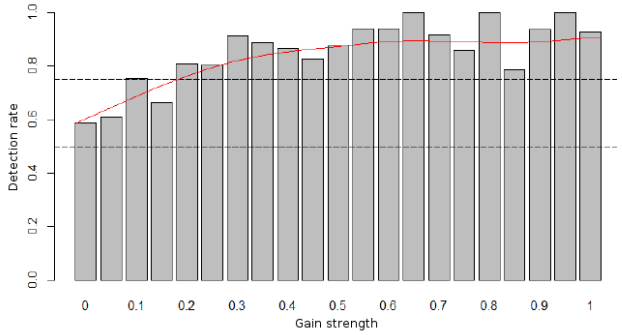

Figure 10: Results of the curvature gain experiments. Positive and negative curvature tests have been combined.

Since the test was designed as a two-alternative forced-choice test, a detection rate of $50\,\%$ indicates the *point of subjective equality* (PSE), because the participants had to give a feedback, either "left" or "right", after each run. A detection rate of $50\,\%$ would then be the result of simply *guessing*.

From the cubic spline drawn in Figs. 10 and 9, the gains for $62.5\,\%$ and $75\,\%$ detection rate can be estimated. The results are summarized in Table 1. The percentual angular ranges for undetected rotations are calculated using Eq. 5. With $R \equiv R_{physical}$, $R - R_\Delta \equiv R_{virtual}$, and $R_{virtual} = 180°$, this equation becomes:

$$R_\Delta = g_R \cdot (180° + R_\Delta) \tag{7}$$

$$R_\Delta = \frac{180°}{1 - g_R} \tag{8}$$

$$\frac{R_\Delta}{R} = \frac{180°}{R \cdot (1 - g_R)} \tag{9}$$

Our results can be compared with similar experiments, to get insight in the role of auditory and visual cues in

Type	Det. rate	Gain	Undetected
Rotation	$75\,\%$	$-0.463 \ldots 0.265$	$-57° \leq R_\Delta \leq 64°$
Rotation	$62.5\,\%$	$-0.366 \ldots 0.150$	$-48° \leq R_\Delta \leq 32°$
Curvature	$75\,\%$	$0.166\,\mathrm{m}^{-1}$	$r \leq 6.024\,\mathrm{m}$
Curvature	$62.5\,\%$	$0.031\,\mathrm{m}^{-1}$	$r \leq 32.3\,\mathrm{m}$

Table 1: RDW detection threshold summary.

RDW. Table 2 compares our data with the results of a visual RDW experiment reported by Steinicke et al. [10], and acoustical RDW experiments by Serafin et al. [2], and by our team [5]. The reported data are transformed to a uniform format and rounded to two significant digits for comparability: Rotational thresholds are given as relative angular manipulations in $\%$ according to Eq. 9, curvature thresholds are given as radii of circles that are perceived as straight paths. All listed data are the $75\,\%$ thresholds in 2AFC-experiments.

Author	Rotation	Curvature
This paper (A + V)	$-32\,\%$ ... $36\,\%$	$6.0\,\mathrm{m}$
Steinicke (V)	$-20\,\%$ ... $49\,\%$	$22\,\mathrm{m}$
Serafin (A)	$-18\,\%$ ... $20\,\%$	$16\,\mathrm{m}$
Our team (A)	$\leq -38\,\%$ ... $18\,\%$	$3.6\,\mathrm{m}$

Table 2: Comparison of RDW detection thresholds with results of other authors. A = acoustic, V = visual RDW control.

When comparing the first and last rows of Table 2, the data tends to contradict the starting hypothesis. It was to be expected that the detection thresholds for the audio-visual experiment (row 1) are higher than the thresholds for the audio-only experiment (row 4), but this is only true for *positive rotation gain* thresholds. For *negative* rotation gains, as well as for *curvature gains*, the gain thresholds are higher in the audio-only experiment.

4.1 Simulator Sickness

Many participants experienced simulator sickness symptoms, especially at higher gain values. In the first 8 runs, some tests even had to be interrupted, when participants complained about nausea. As a consequence, the tests with high gain values were skipped in the subsequent experiments. The average pre-SSQ score was 4.68, the average post-SSQ score was 32.25. The nausea score showed the highest increase, from 2.39 to 42.39. For comparison: In our acoustic RDW experiment, the pre-score was 2.33, and the post-score was 14.0.

A higher SSQ score for the audio-visual experiments had to be expected, since even without manipulations, some people feel uncomfortable watching the virtual scenes of an Oculus Rift.

5. SUMMARY AND OUTLOOK

Experiments to determine detection thresholds for rotational and curvature gains for audio-visual RDW have been car-

ried out. An overview of our results compared to other publications is presented in Table 2. Besides some great variances in the data, a close look shows a slight trend for higher positive rotational gain thresholds when visual cues are present, and for higher curvature gain thresholds with acoustical cues only. From the great variances in experiments of similar type however, it has to be concluded that there are many more factors to be considered, as for instance prior knowledge of the participants, or the consistency of acoustic and visual cues. To shed some light on the latter point, experiments will have to be executed with diverging acoustic and visual gains. As a consequence of the results of Nilsson et al. [13], who did not detect significant differences in their setup (see section 2.5), experiments with more drastic diversions in the acoustical and visual stimuli will be conducted.

Finally, it may be stated that audio-visual redirected walking does not only provide a method to create large virtual spaces in small physical rooms, but it also enables artists to create audio-visual environments that play with the interdependencies of sight, sound, and motion.

6. REFERENCES

[1] E. B. Goldstein, *Sensation and Perception*. Boston, MA: Cengage Learning, 2010.

[2] S. Serafin, N. Nilsson, E. Sikstrom, A. De Goetzen, and R. Nordahl, "Estimation of detection thresholds for acoustic based redirected walking techniques," in *Virtual Reality (VR), 2013 IEEE*, March 2013, pp. 161–162.

[3] J. Lackner, "Induction of illusory self-rotation and nystagmus by a rotating sound-field," *Aviation, space, and environmental medicine*, vol. 48, no. 2, pp. 129–131, February 1977.

[4] S. Razzaque, Z. Kohn, and M. C. Whitton, "Redirected walking," University of North Carolina at Chapel Hill, Chapel Hill, NC, USA, Tech. Rep., 2001.

[5] M. Nogalski and W. Fohl, "Acoustic redirected walking with auditory cues by means of wave field synthesis," in *Proc. 23rd IEEE Conf. on Virtual Reality*. IEEE, March 2016.

[6] J. Dichgans and T. Brandt, "Visual-vestibular interaction: Effects on self-motion perception and postural control," in *Perception*, ser. Handbook of Sensory Physiology, R. Held, H. Leibowitz, and H.-L. Teuber, Eds. Springer Berlin Heidelberg, 1978, vol. 8, pp. 755–804.

[7] E. Hodgson and E. Bachmann, "Comparing four approaches to generalized redirected walking: Simulation and live user data. visualization and computer graphics," *IEEE Transactions on Computer Graphics*, vol. 19, no. 4, pp. 634 – 643, 2013.

[8] P. Lubos, G. Bruder, , and F. Steinicke, "Safe-&-round: bringing redirected walking to small virtual reality laboratories," in *Proc. 2nd ACM symposium of spatial user interaction*. ACM, 2014, pp. 154 – 154.

[9] F. Steinicke, T. Ropinski, G. Bruder, K. Hinrichs, H. Frenz, and M. Lappe, "A universal virtual locomotion system: Supporting generic redirected walking and dynamic passive haptics within legacy 3d graphics applications," in *Virtual Reality Conference, 2008. VR '08. IEEE*, March 2008, pp. 291–292.

[10] F. Steinicke, G. Bruder, J. Jerald, H. Frenz, and M. Lappe, "Estimation of detection thresholds for redirected walking techniques," *Visualization and Computer Graphics, IEEE Transactions on*, vol. 16, no. 1, pp. 17–27, Jan 2010.

[11] ——, "Analyses of human sensitivity to redirected walking," in *Proceedings of the 2008 ACM Symposium on VRST*, ser. VRST '08. New York, NY, USA: ACM, October 2008, pp. 149–156.

[12] V. Pulkki, "Virtual sound source positioning using vector base amplitude panning," *J. Audio Eng. Soc*, vol. 45, no. 6, pp. 456–466, 1997. [Online]. Available: http://www.aes.org/e-lib/browse.cfm?elib=7853

[13] N. C. Nilsson, E. Suma, R. Nordahl, M. Bolas, and S. Serafin, "Estimation of detection thresholds for audiovisual rotation gains," in *Proc. 23rd IEEE Conf. on Virtual Reality*. IEEE, March 2016.

[14] M. Nogalski and W. Fohl, "Acoustically guided redirected walking in a WFS system: Design of an experiment to identify detection thresholds," in *Proc. 12th Sound and Music Computing Conf.* SMC, August 2015.

[15] R. S. Kennedy, N. E. Lane, K. S. Berbaum, and M. G. Lilienthal, "Simulator sickness questionnaire: An enhanced method for quantifying simulator sickness," *The International J. of Aviation Psychology*, vol. 3, no. 3, pp. 203–220, 1993. [Online]. Available: http://ci.nii.ac.jp/naid/30010213408/en/

[16] M. A. J. Baalman, "On wave field synthesis and electro-acoustic music, with a particular focus on the reproduction of arbitrarily shaped sound sources," PhD Thesis, TU Berlin, 2007.

[17] S. Spors and F. Zotter, "Tutorial: Foundations and Practical Aspects of Sound Field Synthesis," http://dx.doi.org/10.13140/RG.2.1.1025.5527, May 2015.

[18] J. Ahrens, *Analytic Methods of Sound Field Synthesis*. Springer Science & Business Media, 2012.

[19] W. Fohl and E. Wilk, "Enhancements to a wave field synthesis system to create an interactive immersive audio environment," in *Proc. 3rd Int. Conf. on Spatial Audio*. VDT, September 2015.